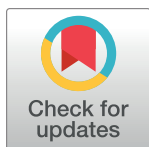


RESEARCH ARTICLE

# CRISPR/FnCas12a-mediated efficient multiplex and iterative genome editing in bacterial plant pathogens without donor DNA templates

Fang Yan<sup>1</sup>✉, Jingwen Wang<sup>1</sup>✉, Sujie Zhang<sup>1,2</sup>✉, Zhenwan Lu<sup>1,2</sup>, Shaofang Li<sup>1</sup>, Zhiyuan Ji<sup>3</sup>, Congfeng Song<sup>4</sup>, Gongyou Chen<sup>5</sup>, Jin Xu<sup>1</sup>, Jie Feng<sup>1</sup>, Xueping Zhou<sup>1,6</sup>, Huanbin Zhou<sup>1,2</sup>\*



**1** State Key Laboratory for Biology of Plant Diseases and Insect Pests, Institute of Plant Protection, Chinese Academy of Agricultural Sciences, Beijing, China, **2** Scientific Observing and Experimental Station of Crop Pests in Guilin, Ministry of Agriculture and Rural Affairs, Guilin, China, **3** National Key Facility for Crop Gene Resources and Genetic Improvement, Institute of Crop Sciences, Chinese Academy of Agricultural Sciences, Beijing, China, **4** Key Laboratory of Monitoring and Management of Plant Diseases and Insects, Ministry of Education, Nanjing Agricultural University, Nanjing, China, **5** State Key Laboratory of Microbial Metabolism, School of Agriculture and Biology, Shanghai Jiao Tong University, Shanghai, China, **6** State Key Laboratory of Rice Biology, Institute of Biotechnology, Zhejiang University, Hangzhou, China

## OPEN ACCESS

**Citation:** Yan F, Wang J, Zhang S, Lu Z, Li S, Ji Z, et al. (2023) CRISPR/FnCas12a-mediated efficient multiplex and iterative genome editing in bacterial plant pathogens without donor DNA templates. PLoS Pathog 19(1): e1010961. <https://doi.org/10.1371/journal.ppat.1010961>

**Editor:** David Mackey, The Ohio State University, UNITED STATES

**Received:** October 30, 2022

**Accepted:** December 27, 2022

**Published:** January 10, 2023

**Copyright:** © 2023 Yan et al. This is an open access article distributed under the terms of the [Creative Commons Attribution License](https://creativecommons.org/licenses/by/4.0/), which permits unrestricted use, distribution, and reproduction in any medium, provided the original author and source are credited.

**Data Availability Statement:** All relevant data are within the manuscript and its [Supporting information](#) files.

**Funding:** This work was supported by grants from the Central Public-interest Scientific Institution Basal Research Fund (No. Y2022QC03) to FY and the Agricultural Science and Technology Innovation Program of the Chinese Academy of Agricultural Sciences to HZ. The funders had no role in study design, data collection and analysis, decision to publish, or preparation of the manuscript.

✉ These authors contributed equally to this work.

✉ Current address: Zhoukou Academy of Agricultural Sciences, Zhoukou, Henan, China

\* [zhouhuanbin@caas.cn](mailto:zhouhuanbin@caas.cn)

## Abstract

CRISPR-based genome editing technology is revolutionizing prokaryotic research, but it has been rarely studied in bacterial plant pathogens. Here, we have developed a targeted genome editing method with no requirement of donor templates for convenient and efficient gene knockout in *Xanthomonas oryzae* pv. *oryzae* (*Xoo*), one of the most important bacterial pathogens on rice, by employing the heterologous CRISPR/Cas12a from *Francisella novicida* and NHEJ proteins from *Mycobacterium tuberculosis*. FnCas12a nuclease generated both small and large DNA deletions at the target sites as well as it enabled multiplex genome editing, gene cluster deletion, and plasmid curing in the *Xoo* PXO99<sup>A</sup> strain. Accordingly, a non-TAL effector-free polymutant strain PXO99<sup>A</sup>D25E, which lacks all 25 *xop* genes involved in *Xoo* pathogenesis, has been engineered through iterative genome editing. Whole-genome sequencing analysis indicated that FnCas12a did not have a noticeable off-target effect. In addition, we revealed that these strategies are also suitable for targeted genome editing in another bacterial plant pathogen *Pseudomonas syringae* pv. *tomato* (*Pst*). We believe that our bacterial genome editing method will greatly expand the CRISPR study on microorganisms and advance our understanding of the physiology and pathogenesis of *Xoo*.

**Competing interests:** I have read the journal's policy and the authors of this manuscript have the following competing interests: The authors have filed a patent application in China based on the results reported in this study. HZ, FY, JW, and SZ, the development and applications of genome editing tools in plant bacterial pathogens. Patent application number: 202210927081.4.

## Author summary

Genetic manipulation of bacterial genomes has greatly advanced our understanding of bacterial physiology and pathogenesis, which further helps us build up cell factories for the production of natural products and breed custom-designed crops for improved disease resistance. Compared with the donor-DNA-mediated homologous recombination methods commonly used in bacterial genome manipulation so far, the donor-DNA-free and CRISPR/Cas-based approaches widely developed in eukaryotic genome editing are more attractive due to their simplicity, versatility, high specificity, and efficiency. However, ectopic expression of Cas proteins causes cell death in many bacterial species, and CRISPR technology has been rarely studied in plant bacterial pathogens. In this work, by co-expressing *mtLigD* and *mtKu* genes, we confirm that the CRISPR/FnCas12a-induced lethal DSBs can be repaired in an error-prone manner, which results in efficient targeted genome editing in both *Xoo* and *Pst* strains. As a result, we have fulfilled various genome editing applications through simple gRNA design and construction, including sequentially knocking out all 25 *xop* genes in *Xoo* PXO99<sup>A</sup> strain, plasmid curing, *etc.* This study highlights the importance and promising application of utilizing heterologous NHEJ proteins in genome editing in microorganisms lacking NHEJ machines in the future.

## Introduction

*Xanthomonas* species, rod-shaped gram-negative bacteria, are well known for their pathogenicity in a wide variety of different plant hosts [1]. Among them, *Xoo* causes bacterial leaf blight (BLB) in rice, which is one of the most severe and prevalent rice diseases causing substantial yield loss during an epidemic in nearly all rice-growing areas, especially in Asian countries. The understanding of the bacterial life cycle, pathogenesis, and colonization in rice will help us breed crops with broad-spectrum resistance and develop bacterial control agents for field application. Also, *Xanthomonas* strains are important resources to produce metabolites for various applications in human society [2]. Therefore, powerful and efficient genetic manipulation methods for *Xanthomonas* are always in great demand. In the past decade, clustered regularly interspaced short palindromic repeats (CRISPR)/CRISPR-associated protein (Cas)-mediated genome editing technology, derived from many bacteria and most archaea, has revolutionized everything from basic science to translational applications related to microorganisms, plants, animals, and human beings [3–8]. However, the application of CRISPR technology in *Xanthomonas* species, or even in plant pathogenic bacteria, has rarely been studied.

Our current knowledge about CRISPR-mediated genome editing in bacteria mainly comes from some human pathogens as well as industrial and laboratory strains, such as *Escherichia coli* [9–11], *Pseudomonas* [12,13], *Mycobacterium* [14], *Bacillus* [15,16], *Corynebacterium* [17], *Clostridium* [18], *Streptomyces* [19], *etc.* Generally speaking, the type II CRISPR/Cas9 system [20] is the most widely-used genome editor in various bacterial strains due to its robust nuclease activity and broad compatibility with other functional proteins (i.e. nucleotide deaminases, transcriptional regulators, DNA polymerase, reverse transcriptase, *etc.*), which facilitates DNA fragment deletion and replacement, nucleotide changes, transcriptional repression and activation of target genes as well as artificial gene evolution [10,21–23]. Alternatively, the type V CRISPR/Cas12a system, characterized by a single crRNA and a thymine-rich protospacer adjacent motif (PAM), is attractive and has been increasingly applied in bacterial genome editing in recent years [20,22,24]. In addition, the type I CRISPR systems, comprising the Cas3

nuclease and multiple effector proteins, have been reprogrammed to edit specific genome regions in its native hosts initially, and further successfully employed in heterologous editing in other bacterium species lacking the natural CRISPR systems [25–27].

The DNA double-strand break (DSB) repair in bacteria is complex and a well-established working model in a given bacterial class cannot be proposed for all bacteria. Anyhow, three different mechanisms, comparable to that in eukaryotes, have been reported in bacteria to date. Among them, homology-directed repair (HDR) is the predominant mechanism for DSB repair in bacteria, which utilizes a homologous template and multi-subunit helicase/nuclease complexes to drive homozygous recombination between the damaged DNA strand and donor, leading to the accurate repair of DSBs [28]. Non-homologous end joining (NHEJ) is a template-independent DSB repair pathway available in only 20–25% of bacteria including *Bacillus subtilis* [28], *M. tuberculosis* [14], *Pectobacterium atrosepticum* [29], *Amycolatopsis mediterranei* [30], etc. Only two proteins, such as the DNA-end-binding protein Ku and a multifunctional ATP-dependent ligase (LigD), are required in the simplified NHEJ machine. In principle, homodimer Ku recognizes and binds to the broken DNA ends, recruiting LigD to rejoin the broken DNA ends in an error-prone way by direct ligation [31,32]. The alternative end joining mechanism (A-EJ; also referred to as microhomology-mediated repair, MMEJ) has been characterized in *E. coli* which lacks NHEJ, it largely relies on the action of RecBCD complex and Ligase-A in the presence of the microhomologies between DSB ends [33]. Overall, DSBs introduced by Cas nucleases in the chromosome are severely toxic to many bacteria and HDR has been widely utilized in combination with donor DNA templates in CRISPR-mediated bacterial genome editing. Accordingly, multiplex genome editing and genome-scale knockout screening are still challenging in bacteria.

The type I-C CRISPR system has been found in genome-sequenced *Xoo* strains worldwide [34,35]. It has been characterized by a set of conserved *Cas* genes and a highly variable CRISPR array. Detailed investigation showed that hijacking the endogenous CRISPR system with an artificial mini-CRISPR array resulted in the self-target killing of the *Xoo* Philippine isolate PXO99<sup>A</sup> [36]. It was most likely due to the unsuccessful DNA repair of Cas3-induced DSBs in PXO99<sup>A</sup>. Indeed, a recent study showed that DSBs caused by *Xoo* CRISPR system could be efficiently repaired by heterologous recombinase ( $\lambda$ -Red) with donor templates, allowing precise genome editing in *Xoo* [37]. Here, to develop an easy-to-use versatile genome editing platform for plant bacterial pathogens, we have comprehensively explored the potential of the CRISPR/Cas12a system from *F. novicida* (FnCas12a) and the crucial NHEJ proteins from *M. tuberculosis* (mtNHEJ) in PXO99<sup>A</sup>. Our data indicate that harnessing both CRISPR/FnCas12a and mtNHEJ achieves highly efficient single and multiple gene knockout, genomic DNA fragment deletion as well as iterative rounds of gene targeting. Also, we validated that our method is suitable for genetic manipulations in another important plant bacterial pathogen *Pst* DC3000 as well.

## Results

### Development of a CRISPR/FnCas12a-based genome editing system in *Xoo* with heterologous NHEJ proteins

To develop a versatile bacterial genome editing system, an intermediate CRISPR construct (termed pHZB3) was designed and generated using an exogenous CRISPR/FnCas12a system instead of the endogenous Cas3 nuclease, in which *FnCas12a* was under the control of the inducible tetracycline promoter to reduce its potential toxicity in bacterial cells and the crRNA was directed by the synthetic constitutive j23119 promoter (Fig 1A). Thus, the 23-nt crRNA protospacers towards TTTV PAM for gene targeting can be easily cloned, and the resulting

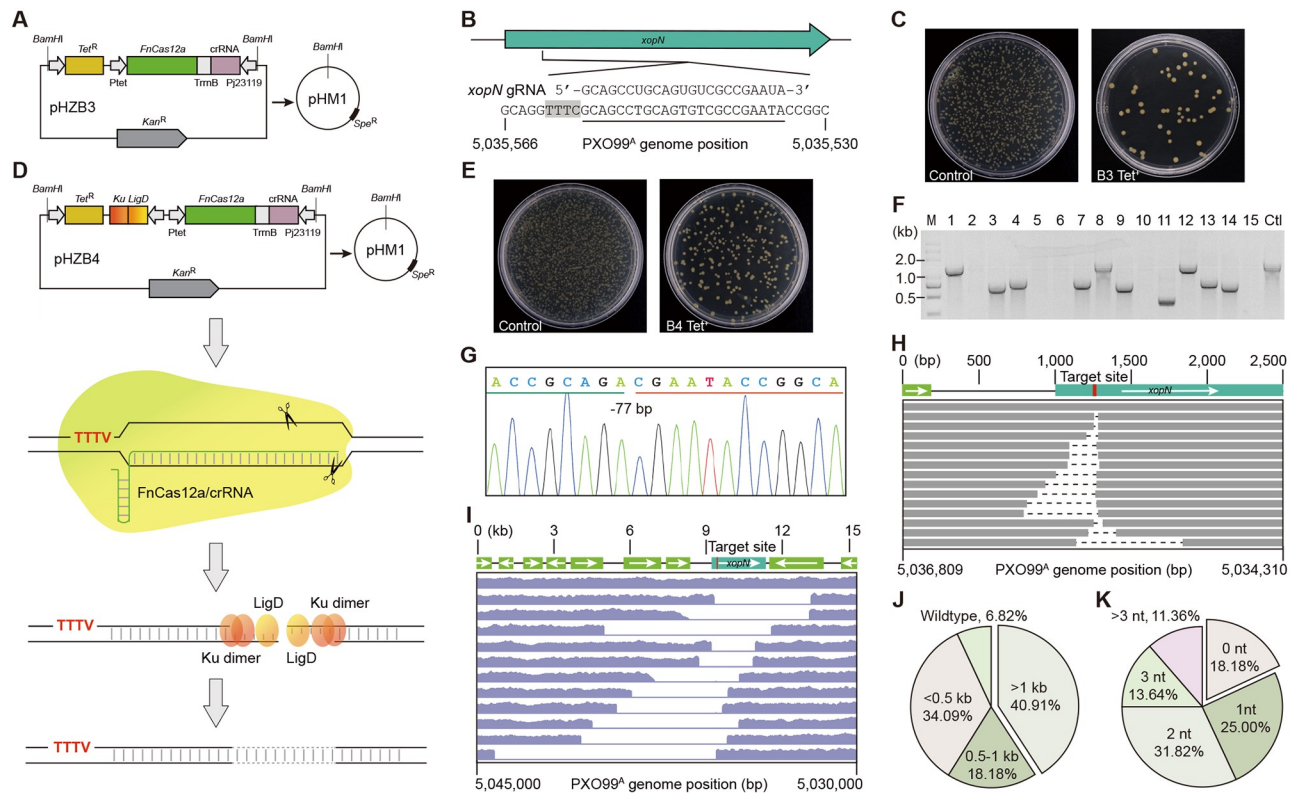


**Fig 1. CRISPR/FnCas12a-mediated genome editing in *Xoo* PXO99<sup>A</sup>.** (A) Schematic illustration of pHM1B3 CRISPR cassette construction. The intermediate CRISPR construct pHZB3 is released through *Bam*HI digestion and integrated into the vector pHM1. *Tet*<sup>R</sup>, tetracycline resistance gene; P<sub>tet</sub>, tetracycline-inducible promoter; FnCas12a, the CRISPR/Cas12a system from *F. novicida*; TrnB, *E. coli* ribosomal RNA terminator rrnB; crRNA, a matured CRISPR RNA; P<sub>j23119</sub>, a synthetic constitutive expression promoter; *Kan*<sup>R</sup>, kanamycin resistance gene; pHM1, a broad-host-range vector; *Spe*<sup>R</sup>, spectinomycin resistance gene. (B) The target site of *xopN*. The target region in PXO99<sup>A</sup> genome is underlined and the PAM sequence is marked by the black shadow. (C) Electroporated PXO99<sup>A</sup> on agar plates. Under the same conditions, except that the control (left plate) did not contain protospacer of *xopN*. (D) Schematic illustration of pHM1B4 CRISPR cassette construction. It's updated from (A) with a single operon encoding mtLigD and mtKu proteins, which reconstitute a simplified non-homologous end joining (NHEJ) machine for DSB repair in *Xoo* cells. (E) As for (C), but showing the genome editing system of pHM1B4. (F) Single colonies in (E) were randomly selected for preliminary identification by PCR amplification of a 1.3-kb genomic fragment flanking the *xopN* gene. M, 5 kb DNA ladder; Ctl, wild-type control. (G) Representative Sanger sequencing chromatogram of the deletion mutant. -77 bp, 77-bp deletion. (H) The deletion size distribution of independent mutant strains was determined by tiling PCR and Sanger sequencing. The first line is wild type, other lines represent independent mutants, the dash lines indicate the deleted region in each mutant, and the target site location is marked in red. (I) As for (H), but determined by the whole-genome sequencing (WGS) analysis of 11 PXO99<sup>A</sup> mutants. (J) The pie chart represents the proportion of different bidirectional deletion ranges. (n = 44 individual colonies randomly selected from (E)). (K) As for (J), but depicting the ratio of the different flanking micro-homology regions used for DSB repair.

<https://doi.org/10.1371/journal.ppat.1010961.g001>

FnCas12a/crRNA-expressing cassettes can be simply released through *Bam*HI digestion and integrated into broad-host-range vectors (i.e., pHM1, pBBR1, etc) for the application in diverse bacteria if wanted. With this CRISPR-Solo strategy, the pHM1B3 construct which carried a gRNA targeting the type III secreted effector (T3SE)-encoding virulence gene *xopN* was electroporated into the *Xoo* strain PXO99<sup>A</sup> (Fig 1B). As shown in Fig 1C, pHM1B3-*xopN*-crRNA yielded a few colonies on agar plates complemented with the transcriptional inducer anhydrotetracycline (aTc). The significant reduction in transformation efficiency of pHM1B3-*xopN*-crRNA compared to that of empty control pHM1B3 indicated that FnCas12a effectively cleaved the bacterial chromosome and the DSB was toxic to the host cells. Twenty-two surviving colonies were randomly picked for genotyping and all were confirmed as wild type, suggesting that native NHEJ and A-EJ are not functional or lacking for DSB repairing in PXO99<sup>A</sup>.



Previous studies showed that mtLigD and mtKu, two crucial NHEJ proteins from *M. tuberculosis*, also function in DNA end-joining in other bacteria, such as *E. coli* and *Corynebacterium glutamicum* [32,38]. We assumed that heterologous mtNHEJ proteins would repair FnCas12a-induced DSBs in *Xoo* cells. Therefore, pHZB3 was upgraded with a single operon of *mtLigD* and *mtKu*, resulting in pHZB4 (Fig 1D). The xopN-crRNA was tested again under the same conditions with the combined CRISPR-NHEJ strategy. As expected, pHM1B4-xopN-crRNA showed greatly increased (~5-fold) transformation efficiency compared to pHM1B3 in repeated experiments (Fig 1E). Forty-four colonies were randomly picked for colony PCR, and the results revealed distinct patterns of genomic deletions at the target site (Fig 1F). Next, tiling PCR and Sanger sequencing were used to determine the flanking sequences of small deletions (Fig 1G and 1H). While for colonies (11) that failed PCR amplification, the whole-genome sequencing (WGS) analysis was performed (Fig 1I). As a result, 41 out of 44 colonies (93.18% editing efficiency) were confirmed with bidirectional deletions ranging in size from 23 bp to 8,808 bp, suggesting that DSBs induced by FnCas12 nuclease are efficiently repaired by the ectopically expressed mtNHEJ proteins. Of note, it was observed that 15 colonies (34.09%) carried small deletions less than 0.5 kb and 18 (40.91%) had fragment deletions larger than 1 kb in size (Fig 1J). In addition, 36 colonies (81.82%) were characterized by flanking microhomology regions ranging from 1 to 7 bp at the breakpoint junctions (Fig 1K), implying that both NHEJ and A-EJ pathways are responsible for DSB repairing in the presence of mtLigD and mtKu in PXO99<sup>A</sup>.

Another T3SE virulence gene, *xopV*, was further targeted using the CRISPR-NHEJ strategy (S1A Fig). Colony PCR and Sanger sequencing analysis showed that pHM1B4-xopV-crRNA achieved comparable transformation efficiency and generated deletions of varying sizes at the target site in 93.18% (41 out of 44 colonies) of randomly-selected colonies (S1B–S1D Fig). Consistent with the finding of pHM1B4-xopN-crRNA, pHM1B4-xopV-crRNA induced both small (< 0.5 kb, 20.45%) and large (> 1 kb, 54.55%) DNA fragment deletions in PXO99<sup>A</sup> after DSB repair via both NHEJ and A-EJ pathways (S1E and S1F Fig). It is important to mention that the dominant occurrence of large deletions was not well correlated to either the amount or induction time of aTc under our assay conditions. Collectively, these data suggest that the combined use of the exogenous CRISPR/FnCas12a system and mtNHEJ proteins enables high-efficiency gene knockout in *Xoo* cells.

### Multiplex genome editing and targeted chromosomal DNA fragment deletions in *Xoo*

We next investigated whether our method could be employed in multiple gene mutagenesis in *Xoo*. Equal amounts of the above-mentioned pHM1B4-xopN-crRNA and pHM1B4-xopV-crRNA were electroporated into PXO99<sup>A</sup> cells simultaneously (Fig 2A). After transformation, only single editing events (small or large deletions) at either *xopN* or *xopV* target sites, but not co-editing events, were detected (Fig 2B and 2C), suggesting that multiple gRNAs should be integrated into the same plasmid for co-editing.

It's well known that FnCas12a is capable of processing its own pre-crRNA into mature crRNAs [24], rendering it a versatile tool for multiplex genome editing in bacteria with a single customized CRISPR array consisting of tandem repeats of 19-nt direct repeat and 23-nt proto-spacer. Therefore, the 23-nt xopN-crRNA and xopV-crRNA were assembled into a crRNA array and electroporated into PXO99<sup>A</sup> cells with the CRISPR-NHEJ strategy. We observed that dual gRNAs caused a dramatic decrease in the number of surviving colonies in repeated experiments, which were likely a result of untimely DSB repair and cell death triggered by large chromosomal excision between *xopN* and *xopV* genes. A total number of 30 colonies was

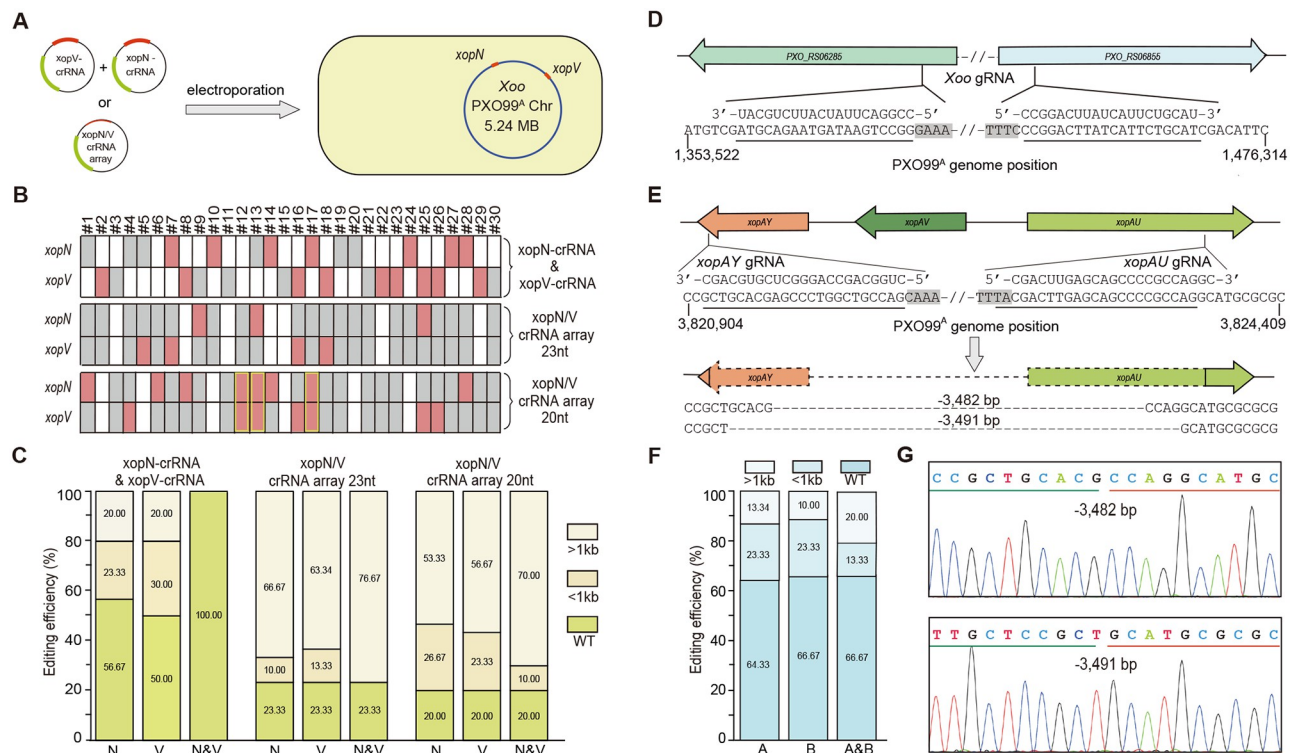


**Fig 2. Multiplex gene knockout and accurate chromosomal DNA fragment deletion in *Xoo PXO99<sup>A</sup>* by CRISPR/FnCas12a.** (A) Schematic illustration of pHM1B4-mediated simultaneous gene editing of *xopN* and *xopV* in *PXO99<sup>A</sup>* with different approaches. Approach I: Equal amounts of plasmid DNA of pHM1B4-*xopN*-crRNA and pHM1B4-*xopV*-crRNA were simultaneously electroporated into *PXO99<sup>A</sup>*. Approach II: A single pHM1B4 plasmid carrying a crRNA array of 20- or 23-nt protospacers was electroporated into *PXO99<sup>A</sup>*. The relative positions of *xopN* and *xopV* genes in the *PXO99<sup>A</sup>* genome (NC\_010717.2) are marked in red. (B) Thirty independent colonies were randomly picked for genotyping by tilling PCR amplification across ~3 kb region around the target sites. Each column represents the identities of *xopN* and *xopV* in a single independent colony. The blank, grey, and red boxes denote wild type, large deletions (>1 kb), and small deletions (<1 kb), respectively. Colonies bearing small deletions in both *xopN* and *xopV* are framed by yellow rectangles. #1–30, colony No.; crRNA-*xopN* & crRNA-*xopV*, *Xoo* cell transformation with two pHM1B4 plasmids (Approach I); *xopN/V* crRNA array, *Xoo* cell transformation with a single pHM1B4 plasmid carrying 20- or 23-nt protospacer (Approach II). (C) Statistical graphics showing the percentage of various deletion mutations in *xopN* and *xopV* in regard to different genome editing approaches. N, *xopN*; V, *xopV*; N&V, *xopN* and *xopV*. Colonies bearing small deletions in both *xopN* and *xopV* were considered as < 1kb category, colonies showing a mixed pattern with both < 1kb and a > 1kb deletions were considered as the >1kb category, and colonies showing a mixed pattern with both wild type and >1kb deletion were considered as the WT category. No co-editing events were detected after transformation in Approach I; Co-editing of both *xopN* and *xopV* with crRNA array of 23-nt protospacers occurred in all positive colonies and resulted in large deletions. (D) Genome editing of two homologous genes (*PXO\_RS06285* and *PXO\_RS06855*) using crRNA with a 20-nt protospacer. (E) Schematic illustration of precise deletion of a 3.84-kb *xopAY*-*xopAU* gene cluster using 23-nt paired gRNAs. Surviving colonies were genotyped by PCR amplification and Sanger sequencing. The sequences below are the junction sequences with the deletions (dashed lines). The target regions are underlined and the PAM sequences are marked by the black shadow in (D) and (E). (F) Statistical graphics showing the percentage of various deletion mutations in *PXO\_RS06285* and *PXO\_RS06855* using approach II (20-nt protospacer). A, *PXO\_RS06285*; B, *PXO\_RS06855*; A&B, both *PXO\_RS06285* and *PXO\_RS06855*. (G) Sanger sequencing chromatograms of the deletion mutants shown in (E). The junction sequences are underlined in different colors (green and red).

<https://doi.org/10.1371/journal.ppat.1010961.g002>

genotyped by PCR amplification of the target regions, and 23 colonies (76.67% efficiency) were identified with deletion mutations (Fig 2B and 2C). Of note, co-editing of both *xopN* and *xopV* occurred in all positive colonies. However, large DNA deletions (PCR amplification failure across the appropriate 3-kb genomic region), instead of small deletions, were observed at all target sites (Fig 2B and 2C). It's well known that the genome editing activity and specificity of various CRISPR/Cas systems are affected by truncated protospacers [24,39,40]. Thus, the original 23-nt protospacers were shortened to 20-nt long in an attempt to attenuate the nuclease activity of FnCas12a/crRNA complex. In this case, timely DSB repair may occur in transformants. The resulting crRNA array was tested under the same conditions as described

above. We observed that 24 out of 30 randomly-selected colonies (80.00% efficiency) had deletions, 3 of which contained small deletions in both *xopN* and *xopV* targets. Building on this finding, another 20-nt gRNA was designed to target a conserved region of two homologous genes, *PXO\_RS06285* and *PXO\_RS06855* which share 91.83% sequence identity in PXO99<sup>A</sup>, and further examined in multiplex genome editing (Fig 2D). Out of 30 randomly-selected colonies, 10 positive colonies (33.33% efficiency) were identified with double gene mutation. Among them, 4 colonies were characterized by small deletions (19–569 bp) in both target genes (Fig 2F). Collectively, these results suggest that the size of deletion mutation in bacterial genome editing could be affected by the activity of CRISPR/FnCas12a system and 20-nt protospacers are likely more suitable for multiplex genome editing in *Xoo*.

Meanwhile, two 23-nt specific gRNAs (*xopAY*-crRNA and *xopAU*-crRNA) were designed to target both ends of a 3.84-kb gene cluster, which encode *XopAY*, *XopAV*, and *XopAU* effectors (Fig 2E), and used to investigate if cleavages of the chromosome would allow the precise deletion of the genomic fragment in PXO99<sup>A</sup>. After electroporation, 19 out of 22 randomly-selected colonies (86.36% efficiency) were identified with target deletions. Among them, 2 colonies were characterized by the accurate excision of 3,482-bp and 3,491-bp fragment, which were derived from the direct end-joining between the two predicted cleavage sites of FnCas12a in *xopAY* and *xopAU* (Fig 2E and 2G).

### Construction of PXO99<sup>A</sup> polymutant strain lacking all 25 non-TAL effectors

Next, we sought to develop a protocol for iterative rounds of genome editing in PXO99<sup>A</sup>, which allows for unlimited stacking of targeted gene knockouts. In this regard, the previously introduced pHM1B4-crRNA plasmid must be eliminated prior to the next round of genome editing. To address this question, a crRNA array containing 2 gRNAs, which individually targeted the oriV replicon of pHM1 and the *mtLigD* gene in pHM1B4, respectively, was designed (S2A Fig) and constructed with the CRISPR-Solo strategy, resulting in pHM1B3-oriV/*mtLigD*-crRNA (namely pHM1B3-VD). Theoretically, both plasmid-curing of any pHM1B4 construct and self-curing of pHM1B3-VD can be simultaneously achieved through one-step transformation of pHM1B3-VD due to the inefficient relegation of linearized plasmids with destroyed *mtLigD* gene and the inability of plasmid propagation with disrupted oriV replicon. pHM1B3-VD was electroporated into the *xopN*-edited PXO99<sup>A</sup> strain harboring the pHM1B4-*xopN*-crRNA plasmid mentioned above and the dynamics of plasmid-curing were investigated with different dosages of aTc at different time points. Spectinomycin sensitivity assay and PCR genotyping indicated that 70–75% of colonies were plasmid-free after 4 to 12-hour induction of the curing system (S2B–S2D Fig). Thus, the application of pHM1B3-VD plasmid enables fast and highly efficient plasmid curing, and the repeated use of pHM1B4-crRNA and pHM1B3-VD constructs allows us to establish a convenient workflow for *Xoo* strain construction (Fig 3A).

The highly virulent *Xoo* strain PXO99<sup>A</sup> encodes 18 transcription activator-like effectors (TALEs) and 25 non-TAL effectors (*Xops*), of which a number of *Xop* proteins (i.e. *XopR*, *XopY*, *XopP*, etc.) have been already confirmed as virulence factors in suppressing immunity to *Xoo* in rice [41–43]. To provide a new research tool to better probe rice-*Xoo* interactions, we aimed to generate a disarmed PXO99<sup>A</sup> polymutant strain lacking all *Xop* effectors through iterative genome editing. Thus, the remaining 24 annotated *xop* genes in the PXO99<sup>A</sup>Δ*xopN* strain were knocked out consecutively to produce PXO99<sup>A</sup>Δ25E strain with small deletions exclusively residing in the coding region of each *xop* gene (Fig 3B). An overview of genome editing of each *xop* and effector gene cluster is provided in Fig 3C, S3 and S4 Figs. In summary,

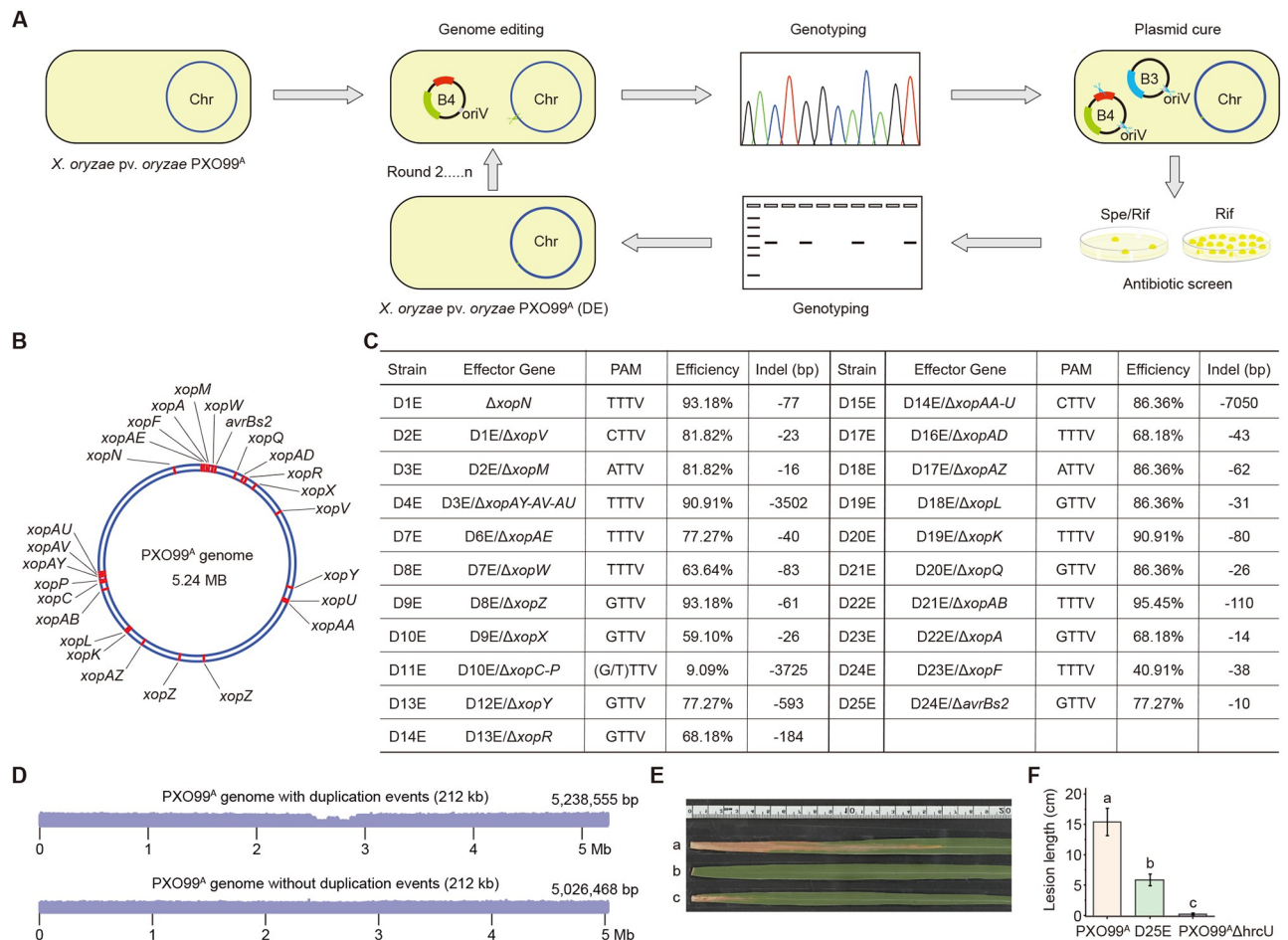


**Fig 3. Iteratively knocking out all 25 non-TAL effector genes in *Xoo* PXO99<sup>A</sup>.** (A) A protocol for iterative rounds of genome editing in PXO99<sup>A</sup>. The pHM1B4 plasmid was transformed into PXO99<sup>A</sup> competent cells by electroporation. Surviving colonies were genotyped by Sanger sequencing of the targeted gene, and then the mutant strains that meet the requirements were selected for plasmid-curing. Determination of successful plasmid elimination was done by screening in media and PCR assay, and a plasmid-free mutant was used for the next round of knockout operations. Spe, spectinomycin; rif, Rifampicin. (B) The positions of all 25 non-TAL effectors in the PXO99<sup>A</sup> genome (NC\_010717.2) are marked in red. (C) The table shows the name, target gene(s), PAM sequence, efficiency, and deletion size of the *xop* mutants obtained in each round of genome editing. (D) Genome-wide coverage of PXO99<sup>A</sup> when aligned back to the genome with the 212 kb duplication event (top) and the genome without the 212 kb duplication event (bottom). (E) Disease phenotypes of Kitaake after inoculation with *Xoo* strains. a, PXO99<sup>A</sup>; b, PXO99<sup>A</sup>ΔhrcU; c, PXO99<sup>A</sup>ΔD25E. (F) Disease lesion lengths on Kitaake. Lesions were measured 14 days post inoculation. All values represent means  $\pm$  s.d. (n = 8, 5 replicates). Values with different letters significantly differ from each other (Tukey's test, P < 0.05).

<https://doi.org/10.1371/journal.ppat.1010961.g003>

the CRISPR-NHEJ strategy resulted in high editing frequencies ranging from 40.91 to 95.45% when a single gRNA was used to target each *xop* gene in each round (Fig 3C). As for the other *xops* arranged in gene clusters, the crRNA arrays achieved DNA fragment deletion efficiency of 90.91%, 9.09%, and 86.36% for *xopAY-AV-AU*, *xopC-P*, and *xopAA-U*, respectively (Fig 3C). Notably, since crRNAs for four types of NTTV PAMs (ATTV, CTTV, TTTV, and GTTV) were included and had high editing efficiency, our data indicate that CRISPR/FnCas12a recognizes TTV PAM in *Xoo* cells, in contrast to other bacteria. Overall, our iterative genome editing system facilitates *Xoo* strain construction with simple gRNA manipulations compared to homologous donor-mediated traditional methods.

Furthermore, the PXO99<sup>A</sup>ΔD25E strain was subjected to WGS analysis to evaluate the genome-wide off-target DNA mutations induced by FnCas12a nuclease. Besides the identified



on-target DNA deletions in 25 *xop* genes, 3 single nucleotide polymorphisms (SNPs) and two small indels (1-nt deletion and 7-nt insertion) were detected in the PXO99<sup>A</sup>D25E genome (S5 Fig). Among these off-target sites, only 1 SNP was located in the coding region, resulting in the substitution of asparagine with aspartic acid (N2D) of RS25085 (S5D Fig). Given the occurrence of 5 crRNA-independent mutations (likely to be spontaneous mutations) in 42 times of FnCas12a-mediated editing, including both gene targeting and plasmid cure, we presume that FnCas12a nuclease with stringently-designed protospacer does not cause obvious off-target mutations in bacterial genome editing. In addition, when aligning those sequencing reads to the *xopZ*-resided 212-kb duplication region [44] in the reference genome of PXO99<sup>A</sup>, we revealed that there was only one copy of *xopZ* existing in our PXO99<sup>A</sup> and PXO99<sup>A</sup>D25E strains (Fig 3D). Finally, we inoculated rice variety Kitaake with PXO99<sup>A</sup>D25E, PXO99<sup>A</sup>, and the type III secretion system (T3SS)-deficient PXO99<sup>A</sup>ΔhrcU mutant which is unable to deliver T3SEs. The lesion length caused by PXO99<sup>A</sup>D25E was significantly decreased compared to PXO99<sup>A</sup>, but slightly higher than PXO99<sup>A</sup>ΔhrcU (Fig 3E and 3F), highlighting the critical virulence function of the non-TAL effector repertoire in the pathogenesis of PXO99<sup>A</sup> on rice.

### Application of CRISPR/FnCas12a in *Pst*

We also investigated the CRISPR-NHEJ strategy in genome editing in *Pst*, which is another intensively studied bacterial pathogen in dicot plants but does not bear any native CRISPR/Cas system. A gRNA was designed to target the T3SE gene *hopAB2* residing on the circular chromosome (Fig 4A and 4B). The pHZB4 intermediate carrying *hopAB2*-crRNA was integrated into broad-host-range vectors pBBR1MCS-2 in this case and the resulting pBBR1B4-*hopAB2*-crRNA construct was electroporated into *Pst* DC3000. As observed, CRISPR/FnCas12a also resulted in decreased transformation efficiency of *Pst* DC3000, which is comparable to PXO99<sup>A</sup>. Twenty-two colonies were randomly picked from 46 colonies for genotyping and 8 colonies (36.37% efficiency) were identified with fragment deletions of various sizes at the target site. Sanger sequencing analysis of small deletions further verified the occurrence of 438 to 714-bp deletions in *hopAB2* (Fig 4C). These data indicate that the combined use of the exogenous CRISPR/FnCas12a system and mtNHEJ proteins enables efficient gene knockout in *Pst* as well.

Considering that native plasmids in many *Pst* strains are important or essential for host-pathogen interactions and the fast plasmid-curing methods are always attractive to researchers, we next employed a gRNA to target *hopX1*, which encodes another T3SE but is present on the 73-kb native plasmid pDC3000A (Fig 4D and 4E), in an attempt to remove pDC3000A with the CRISPR-Solo strategy. After electroporation, pBBR1B3-*hopX1*-crRNA yielded a large number of colonies of *Pst* DC3000. Colony PCR was performed using 4 pairs of primers to examine the presence/absence of plasmid pDC3000A and pBBR1B3, and the identity of the DC3000 chromosome, respectively, in 22 randomly-selected colonies (Fig 4D). As a result, pDC3000A was eliminated in 100% of the *Pst* cells (Fig 4F), suggesting that CRISPR/FnCas12a nuclease enables high-efficiency curing of native plasmids in *Pst* in one-step transformation.

### Discussion

In the past decade, great efforts have been invested in developing donor-free CRISPR-mediated genome editing technologies in *X. oryzae*, but the strong lethal effect of CRISPR in *Xoo* and the poorly characterized genetic background of PXO99<sup>A</sup> make it challenging. In this study, we have successfully built up a stable CRISPR/FnCas12a-based genetic manipulation platform (CRISPR-Solo and CRISPR-NHEJ) in *Xoo*, achieving an average efficiency of

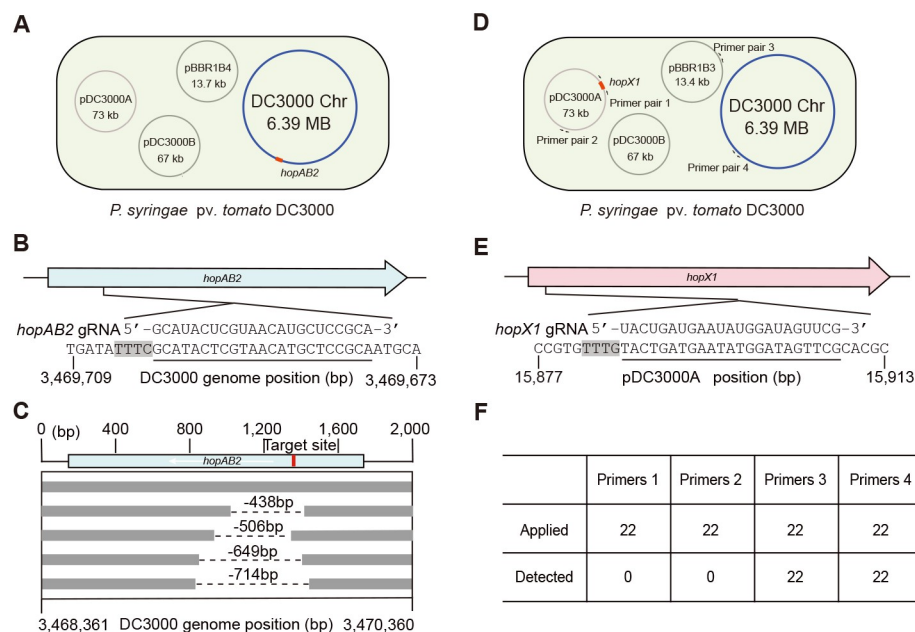


**Fig 4. CRISPR/FnCas12a-mediated genome editing in *Pst* DC3000.** (A) Schematic illustration of pBRR1B4-mediated gene knockout of *hopAB2* residing on the circular chromosome in *Pst* DC3000. The relative position of *hopAB2* on the chromosome is marked in red. (B) The target site of *hopAB2*. (C) Deletions detected in *hopAB2* knockout mutants by colony PCR and Sanger sequencing. Each line represents an independent mutant, the dashed lines indicate the deleted region in each mutant, and the target site location is marked in red. (D) Schematic illustration of pBRR1B3-mediated pDC3000A plasmid curing of *Pst* DC3000 by targeting *hopX1*. The relative positions of *hopX1* on pDC3000A and PCR amplification regions are shown in red and by arrows, respectively. The primer sequences are listed in the S3 Table. (E) The target site of *hopX1*. (F) Summary of the plasmid-curing frequency using 22 randomly-selected colonies and primer pairs shown in (D). The target regions are underlined and the PAM sequences are marked by the black shadow in (B) and (E), respectively.

<https://doi.org/10.1371/journal.ppat.1010961.g004>

appropriate 78% for single gene targeting. It allows us to further perform convenient multiplex gene targeting, gene cluster deletion as well as iterative genome editing as expected. Also, we verified that both strategies are suitable for relevant genetic manipulation in *Pst*.

Before this study, the marker exchange strategy and the suicide-vector-mediated non-marker mutagenesis method have been extensively used for gene disruption through homologous recombination in *X. oryzae* [45,46]. It requires the stringent design of homology templates, complex construction of vectors, and large-scale screen for the 2<sup>nd</sup> crossover recombination event sometime. Even more, this strategy failed to disrupt certain genes for an unknown reason. Recently, an efficient genome editing approach using the endogenous type I-C CRISPR/Cas system of *Xoo* and the  $\lambda$ -Red recombinase system was reported, it needs the construction of both a mini-CRISPR array and a homologous template [37]. By contrast, the CRISPR-NHEJ strategy that we developed offers a template-free, user-friendly, and more robust way for targeted gene knockout in *Xoo*. Using the updated pHM1B4 vector (CRISPR and mtNHEJ modules are directly assembled in pHM1), a single protospacer or crRNA array can be rapidly cloned even within 2 days by simple manipulation of oligonucleotides, and it is effective in the editing of all target genes tested in our study.

Another obvious advantage of the donor-free CRISPR-NHEJ strategy is its potential and application in the co-editing of multiple target sites in the *Xoo* genome using crRNA arrays, such as simultaneously editing of two genes with 20-nt protospacers and deletion of gene clusters with 23-nt protospacers. It facilitates generating polymutant strains for studying gene

family, metabolic pathways, and signaling cascades, and minimizing bacterial genomes to explore the pan-genome and evolution of *Xoo*, respectively. To be mentioned, different from our observation on rice, zero or very few transformants escaped from editing were obtained in our attempt to simultaneously edit all 18 TALE encoding genes in PXO99<sup>A</sup> with a crRNA array, which implies that *Xoo* cell cannot tolerate a large number of chromosome cleavages. In this regard, the CRISPR-NHEJ strategy could be further updated by enhancing the repair capacity of heterologous DNA repair machines, such as using codon-optimized NHEJ genes, employing NHEJ proteins from other bacterial species, artificially engineering NHEJ proteins for high-activity variants, *etc.*, or developing multiplex base editing [47,48] which disrupt target genes through induction of STOP codons without causing any double-stranded DNA cleavage.

The CRISPR-NHEJ strategy dominantly produces DNA fragment deletions (23 bp to 8 kb deletion in *Xoo* and >438 bp deletion in *Pst* in our study) other than insertions at regions of microhomology (1~7 bp), we reason that the output of genome editing using our method is highly correlated to the distribution of direct microhomologous repeats flanking the cleavage site on the genomic DNA in different bacterial species. Anyhow, the occurrences of both small and large deletions in *Xoo* genome editing allow us to disrupt the target genes precisely without affecting overlapping open reading frames and nearby genes.

Besides *Xoo*, the CRISPR-mediated technologies for plasmid curing, gene knockout, and base editing have been preliminarily explored in only a few other bacterial plant pathogens, including *Pst* [25,49], *P. syringae* pv. *actinidiae* (*Psa*) [50], *Pseudomonas chlororaphis* [51], *Agrobacterium* spp. [52], and *Erwinia amylovora* [53]. Regarding gene knockout, the ectopic expression of the type I-C CRISPR/Cas3 system from *P. aeruginosa* in *Pst* DC3000 resulted in 67–92% efficiency of genome editing, characterized by large deletions (55–100 kb) at four target sites [25]; Application of CRISPR/SpCas9 in *Psa* generated very few transformants with one targeting sgRNA and 64.29% positive colonies carried 7.82–64 kb deletions. It's important to note that most of these deletions in both reports were flanked by microhomologous sequences. Combined with our data, it highlights that the CRISPR/Cas nuclease-induced cleavages in the bacterial chromosomes are repaired, but not in time, through the native A-EJ pathways when NHEJ is lacking, and introducing heterologous NHEJ into genome editing (the CRISPR-NHEJ strategy) in phytopathogenic bacteria can increase the transformation efficiency as well as reduce the size of deletion mutations. we propose that our CRISPR-NHEJ strategy presented in this study is suitable for direct application or developing the relevant tools in other bacterial species, even in other microorganisms.

Transposon-based large-scale mutagenesis has been broadly performed for genetic and molecular analysis in plant bacterial pathogens, but their transposition has insertion bias and is not nearly random in the bacterial genomes [54–56]. By contrast, CRISPR tools enable us to perform more robust genome-scale screens in a custom way in bacteria at a low cost. Before our study, a large-scale CRISPR interference (CRISPRi) approach, which uses dCas proteins to temporarily knock down the target gene expression, has been developed considering the high toxicity of Cas nucleases [6]. Technically, our high-efficiency CRISPR-NHEJ strategy, which knocks out target genes specifically, opens the prospect of genome-scale mutagenesis in bacteria, it provides a mechanistically distinct method from CRISPRi for systematic genetic analysis.

One of the important outcomes of our work is the iterative genome editing method with well-designed gRNAs in *Xoo*, it enables the construction of chassis strains (i.e., PXO99<sup>A</sup>D25E, *etc.*) for probing functionally redundant effectors and plant innate immune system as well as “build-your-own” cell factories for producing metabolites (i.e., xanthan gum, *etc.*). A DNai technique, which was based on the CRISPR/Cas3-mediated targeted degradation of DNA, was

established to degrade a user-specified set of DNA targets for trade secrets and environment control [57]. Here we showed that the FnCas12a-mediated CRISPR-Solo strategy caused severe cell death of *Xoo* or achieved high-efficiency elimination of heterologous plasmids in *Xoo* and endogenous plasmid in *Pst* depending on the residence of the target site. In light of these findings, we claim that our CRISPR-Solo strategy could be also applied to the protection of engineered *Xoo* cell factories in commercial use and control of potentially hazardous material release into the environment by using tight regulators and multiple protospacers. What's more, the CRISPR-Solo strategy, combined with various conjugative systems [58], might be potentially applied to manipulate the soil bacterial diversity for biological improvement and control.

In conclusion, a donor-free, high-efficiency, targeted gene knockout method has been well established in bacterial plant pathogens by employing both inducible CRISPR/FnCas12a system and heterologous mtNHEJ proteins in this study. It enables us to conveniently construct bacterial strains regardless of target gene numbers as well as large-scale gene knockout screens regardless of the presence/absence of endogenous end joining repair machines. Our detailed study gives novel insights into the development of targeted genome editing technologies in diverse microorganisms, and undoubtedly accelerates both the fundamental study and applied biological control research in plant pathology as well as the metabolic engineering of *Xanthomonas* in the industry.

## Materials and methods

### Bacterial strains, plasmids and primers

All bacterial strains and plasmids used in the study along with their relevant characteristics and source are described in [S4 Table](#). Primers used for plasmid construction and PCR amplifications are provided in [S3 Table](#).

### Bacterial growth conditions

*X. oryzae* pv. *oryzae* strains were grown in Nutrient Broth (NB, Nutrient Broth, Difco, BD, 8g/L) or Nutrient Broth plate supplemented with 1.5% agar (NA) at 28°C. *P. syringae* pv. *tomato* strains were grown in King's B (KB) medium (Protease peptone No.3 20g/L, K<sub>2</sub>HPO<sub>4</sub> 1.5g/L, Glycerol 15g/L, with or without 1.5% agar, add 3.2 mL of 1M MgSO<sub>4</sub> after autoclaved) at 28°C. *E. coli* strains were grown in Luria Bertani (LB) media with or without 1.5% agar at 37°C. Antibiotics were used at the following final concentrations unless otherwise noted: Ampicillin (Amp), 50 µg/ml; Spectinomycin (Spe), 100 µg/ml; Kanamycin (Kan), 50 µg/ml; Anhydrotetracycline (aTc), 200 µg/ml; Rifampin (Rif), 50 µg/ml.

### Plasmid construction

The 4,394-bp fragment consisting of *FnCas12*-expression cassette and crRNA-expression cassette was codon-optimized for suitable expression in PXO99<sup>A</sup> and synthesized by Sangon Biotech (Shanghai, China) ([S1 Table](#)). The 4,394-bp fragment digested by *Acc65I*/*SpeI* (Thermo Scientific) was cloned into the vector backbone of pENTR4-gRNA4 which was amplified with the primer pair pENTR4-F1/pENTR4-R1 and Phanta Max Super-Fidelity DNA Polymerase (Vazyme, China), resulting in pENTR4-FnCas12a. Tet<sup>R</sup> (the repressor of the tetracycline resistance element) insertion was performed by ClonExpress II One Step Cloning Kit (Vazyme, China) with *SpeI*-digested pENTR4-FnCas12a and Tet<sup>R</sup> amplicon of plasmid pFREE vector (Addgene, #92050) with the primer pair Tet-F3/Tet-R3, resulting in pHZB3. The *mtLigD*/*mtKu*-expression cassette was codon-optimized for suitable expression in PXO99<sup>A</sup>,



synthesized by Sangon Biotech (Shanghai, China) (S1 Table), and then inserted into the pHZB3 through *SpeI* digestion and DNA ligation, resulting in pHZB4.

For the construction of FnCas12a/crRNA plasmids, the 26-nt or 23-nt complementary oligos corresponding to each target site (S3 Table) and carrying appropriate 3-nt adaptor were phosphorylated, annealed, and inserted into the *SapI*-digested pHZB3 or pHZB4, resulting in pHZB3-crRNA or pHZB4-crRNA, respectively. Similarly, crRNA arrays, composed of tandem repeats of 19-nt direct repeat and 23-nt or 20-nt protospacer, were synthesized by Sangon Biotech (S3 Table) and inserted into the *SapI*-digested pHZB3 or pHZB4 as described above.

Next, the FnCas12a/crRNA-expression cassettes in pHZB3 and pHZB4 were cloned into pHM1 vector through *BamHI* digestion and DNA ligation, resulting in pHM1B3-crRNA and pHM1B4-crRNA for genome editing in PXO99<sup>A</sup> strains, respectively. Similarly, the FnCas12a/crRNA-expression cassettes were cloned into pBBR1MCS-2 to generate pBBR1B3-crRNA and pBBR1B4-crRNA for genome editing in *Pst* DC3000 strains, respectively.

### Competent cell preparation and electroporation

The plasmids used in this study were delivered into *Xoo* PXO99<sup>A</sup> and *Pst* DC3000 by electroporation. Electro-competent cell preparation and electro-transformation were performed as follows. 1-mL overnight culture of PXO99<sup>A</sup> was 1:10 diluted into 10 mL of fresh medium and incubated at 28°C until OD<sub>600</sub> reaches 0.7–1.0. The cells were harvested by centrifugation at 5,000g for 10 min. The supernatant was discarded and the cells were washed twice with 10 mL of chilled, sterile MilliQ water at 4°C. Finally, the cells were resuspended in 1 mL (1/10 original volume) of 10% glycerol and divided into 100 µL aliquot for the subsequent experiments.

The plasmids were transformed into PXO99<sup>A</sup> by electroporation with the parameters of 2500 V, 2 mm cuvette (Bio-Rad). The mixture was recovered for 2–3 h in 1 mL of NB medium at 28°C and then cultured for 2 h after adding aTc to a final concentration of 200 µg/mL. The colonies containing pHM1 were selected on NA plates containing 100 µg/mL Spe. Similar procedures were performed to prepare DC3000 electrocompetent cells and transformation using KB medium.

### Plasmid curing

*Xoo* PXO99<sup>A</sup> strains harboring various pHM1B4-crRNA plasmids were grown in 10 mL of NB complemented with 100 µg/ml Spe to prepare electrocompetent cells. 200 µL of competent cells were transformed with 1 µg of pHM1B3-VD plasmid by electroporation and recovered for 2–3 hours in 2 mL of NB medium at 30°C with shaking. After that, a gradient of the final concentration of aTc (200 ng/mL, 500 ng/mL, 1000 ng/mL, 2000 ng/mL, 3000 ng/mL) was added, and cell cultures at different induction time points (1, 2, 4, 6, 8, 10, and 12 hours) were plated on non-selective NA plates. A number of colonies for each sample were grown on NA plates with/without Spe. Loss of the plasmids was verified by loss of Spe resistance. Plasmid-free colonies were further confirmed by PCR amplification of the pHM1 backbone.

### DNA extraction and PCR genotyping

Bacterial genomic DNA was isolated from each sample using the SteadyPure Bacteria Genomic DNA Extraction Kit (Accurate Biotechnology Co., Ltd, China) according to the manufacturer's protocol. Tilling PCR amplification across the targeted genomic region was carried out with 2×Taq Master Mix (Vazyme, China) with specific primers listed in S3 Table, the size of PCR products is 1–1.5 kb. Shifted gel bands of PCR products were subjected to Sanger sequencing for identifying mutations. As for the colonies with no PCR product, genomic DNAs were subjected to WGS.

## Whole-genome sequencing library construction and data analysis

RNA-free PXO99<sup>A</sup> genomic DNAs (0.2 µg) were used to construct the DNA libraries using a NEBNext Ultra DNA Library Prep Kit for Illumina (NEB, USA) following the manufacturer's instructions. DNA libraries were sequenced on the Illumina platform in the 150-nt paired-end mode with around 200X coverage.

The sequencing reads were mapped to PXO99<sup>A</sup> genome downloaded from NCBI (NC\_010717.2) via BWA [59] and sorted using samtools (v1.9) [60]. In addition, the genome without the large 212 kb duplication was created by removing the DNA sequence fragment between 2,502,622–2,714,708 [35]. Genome-wide coverage was calculated using in-house python program. The Genome Analysis Toolkit (GATK v4.2) was used to mark duplicated reads and recalibrate base qualities [61]. To identify high-quality genetic changes at the genomic scale, we applied three independent germline variant-calling methods: GATK, LoFreq [62], and Strelka2 [63]. SNPs and indels identified through all three methods were combined together and shown in IGV browser [64].

## Rice growth, inoculation, and statistical analysis

Rice plants of the *Geng* cultivar Kitaake were grown in a growth chamber under the following conditions: 30/25°C (day/night) and 75% relative humidity and a photoperiod of 12 h in light/dark. Fully expanded leaves were inoculated with bacterial suspensions (OD<sub>600</sub> = 0.5) at the four-leaf seedling stage using the leaf-tip-clipping method. Disease symptoms were scored by measuring lesion length 2 weeks post-inoculation (DPI). The statistical significance between samples was analyzed by Tukey's test ( $p < 0.05$ ).

## Supporting information

### S1 Fig. Targeted gene editing of *xopV* in *Xoo* PXO99<sup>A</sup> with the CRISPR-NHEJ strategy.

(A) The target site of *xopV*. The target region in the PXO99<sup>A</sup> genome is underlined and the PAM sequence is marked by the black shadow. (B) Single colonies were randomly selected for preliminary identification by PCR amplification of a 1.1 kb genomic fragment flanking the *xopV* gene. M, 5 kb DNA ladder; Ctl, control. (C) Representative Sanger sequencing chromatogram of the deletion mutant. -201bp, 201-bp deletion. (D) Deletion size distribution of mutants determined using tiling PCR and Sanger sequencing. The first line is wild type, other lines represent independent mutants, the dashed line in the middle indicates the deleted portion of each mutant, and the target site location is marked in red. (E) The pie chart represents the proportion of different bidirectional deletion ranges. (n = 44 individual colonies randomly selected). (F) As for (E), but depicting the ratio of the different flanking micro-homology regions used for DSB repair. (TIF)

### S2 Fig. Fast and efficient curing of exogenous plasmids in *Xoo* PXO99<sup>A</sup> with the CRISPR-solo strategy.

(A) CRISPR/FnCas12a nuclease-mediated cleavages of both oriV replicon and *mtLigD* gene resulted in the simultaneous removal of pHM1B3 and pHM1B4 plasmids. A crRNA array was designed to target the oriV replicon of pHM1 and the *mtLigD* gene in pHM1B4, respectively. The target regions in plasmids are underlined and the PAM sequences are marked by the black shadow. The expression cassettes of *FnCas12a/xopN*-crRNA, *mtKu/mtLigD*, and *FnCas12a/oriV/mtLigD*-crRNA are depicted as yellowgreen, red, and deepsky-blue stripes. B3, pHM1B3-VD plasmid; B4, pHM1B4-crRNA plasmid. (B) Selection of the plasmid-free PXO99<sup>A</sup>Δ*xopN* strains on NB plates with/without spectinomycin after pHM1B3-VD transformation. Spe<sup>-</sup>, without spectinomycin; Spe<sup>+</sup>, with spectinomycin added.

(C) Representative agarose image for the presence/absence of pHM1 plasmid in the PXO99<sup>Δ</sup>*xopN* strain. Colony PCR was performed with pHM1-specific primers and negative PCR result indicated that the colonies were plasmid-free. M, 5 kb DNA ladder; Ctl, control. (D) Time course characterization of the pHM1B3-VD plasmid-curing system in PXO99<sup>Δ</sup>*xopN* cells bearing pHM1B4-*xopN*-crRNA. The percentage of plasmid-free cells was calculated at induction time 1, 2, 4, 6, 8, 10, 12 h after treatment of aTc in different dosages (200–3,000 ng/ml). (TIF)

**S3 Fig. Mutation information on *xop* genes in the PXO99<sup>Δ</sup>D25E strain generated by iterative genome editing.** Specific gRNAs were designed to target *xopV* (A), *xopM* (B), *xopAE* (C), the *xopAY-AV-AU* gene cluster (D), *xopW* (E), the *xopC-P* gene cluster (F), *xopX* (G), *xopY* (H), *xopR* (I), and the *xopAA-U* gene cluster (J), and the CRISPR/FnCas12a-induced deletions are shown in Sanger sequencing chromatograms, respectively. The target regions in the PXO99<sup>Δ</sup> genome are underlined and the PAM sequences are marked by the black shadow. (TIF)

**S4 Fig. Mutation information on *xop* genes in the PXO99<sup>Δ</sup>D25E strain generated by iterative genome editing (continued).** Specific gRNAs were designed to target *xopAD* (A), *xopAZ* (B), *xopL* (C), *xopK* (D), *xopQ* (E), *xopAB* (F), *xopA* (I), *xopF* (G), *avrBs2* (H), and *xopZ* (J), and the CRISPR/FnCas12a-induced deletions are shown in Sanger sequencing chromatograms, respectively. The target regions in the PXO99<sup>Δ</sup> genome are underlined and the PAM sequences are marked by the black shadow. Two identical copies of *xopZ* have been annotated in the reference genome of PXO99<sup>Δ</sup> (NC\_010717.2). (TIF)

**S5 Fig. Off-target analysis of the Xoo PXO99AD25E strain using WGS.** IGV genome browser views show 1-bp deletion (A), 7-bp insertion (B), and A-to-G (C), A-to-C (D), and C-to-G (E) nucleotide substitutions detected at 5 loci in the PXO99<sup>Δ</sup>D25E strain. (TIF)

**S1 Table. The complete nucleotide sequences of the codon-optimized *FnCas12a* and *mtLigD/mtKu* fragments.** (XLSX)

**S2 Table. Target gene list for genome editing in this study.** (XLSX)

**S3 Table. Oligonucleotides used in this study.** (XLSX)

**S4 Table. Bacterial strains and plasmids used in this study.** (XLSX)

## Acknowledgments

The authors thank Dr. Houxiang Kang for help in data analysis, Dr. Bin Ren for assistance in the pathogen inoculation experiment, and Dr. Hailei Wei for providing pBBR1MCS-2 plasmid.

## Author Contributions

**Conceptualization:** Congfeng Song, Gongyou Chen, Jie Feng, Xueping Zhou, Huanbin Zhou.

**Investigation:** Fang Yan, Jingwen Wang, Sujie Zhang, Zhenwan Lu, Shaofang Li.

**Resources:** Zhiyuan Ji, Congfeng Song, Gongyou Chen, Jin Xu.

**Supervision:** Huanbin Zhou.

**Writing – original draft:** Fang Yan, Sujie Zhang, Huanbin Zhou.

**Writing – review & editing:** Huanbin Zhou.

## References

1. Timilsina S, Potnis N, Newberry EA, Liyanapathirana P, Iruegas-Bocardo F, White FF, et al. *Xanthomonas* diversity, virulence and plant-pathogen interactions. *Nat Rev Microbiol*. 2020; 18(8): 415–427. <http://doi.org/10.1038/s41579-020-0361-8> PMID: 32346148.
2. Berninger T, Dietz N, Lopez OG. Water-soluble polymers in agriculture: xanthan gum as eco-friendly alternative to synthetics. *Microb Biotechnol*. 2021; 14(5): 1881–1896. <http://doi.org/10.1111/1751-7915.13867> PMID: 34196103.
3. Zhu H, Li C, Gao C. Applications of CRISPR-Cas in agriculture and plant biotechnology. *Nat Rev Mol Cell Biol*. 2020; 21(11): 661–777. <http://doi.org/10.1038/s41580-020-00288-9> PMID: 32973356.
4. Komor AC, Badran AH, Liu DR. CRISPR-based technologies for the manipulation of eukaryotic genomes. *Cell*. 2017; 169(3): 559. <http://doi.org/10.1016/j.cell.2017.04.005> PMID: 28431253.
5. Hsu PD, Lander ES, Zhang F. Development and applications of CRISPR-Cas9 for genome engineering. *Cell*. 2014; 157(6): 1262–1278. <http://doi.org/10.1016/j.cell.2014.05.010> PMID: 24906146.
6. Todor H, Silvis MR, Osadnik H, Gross CA. Bacterial CRISPR screens for gene function. *Curr Opin Microbiol*. 2021; 59: 102–109. <http://doi.org/10.1016/j.mib.2020.11.005> PMID: 33285498.
7. Nambiar TS, Baudrier L, Billon P, Ciccio A. CRISPR-based genome editing through the lens of DNA repair. *Mol Cell*. 2022; 82(2): 348–388. <http://doi.org/10.1016/j.molcel.2021.12.026> PMID: 35063100.
8. Klanschnig M, Cserjan-Puschmann M, Striedner G, Grabherr R. CRISPRactivation-SMS, a message for PAM sequence independent gene up-regulation in *Escherichia coli*. *Nucleic Acids Res*. 2022; 50(18): 10772–10784. <http://doi.org/10.1093/nar/gkac804> PMID: 36134715.
9. Fang L, Fan J, Luo S, Chen Y, Wang C, Cao Y, et al. Genome-scale target identification in *Escherichia coli* for high-titer production of free fatty acids. *Nat Commun*. 2021; 12(1): 4976. <http://doi.org/10.1038/s41467-021-25243-w> PMID: 34404790.
10. Tong Y, Jorgensen TS, Whitford CM, Weber T, Lee SY. A versatile genetic engineering toolkit for *E. coli* based on CRISPR-prime editing. *Nat Commun*. 2021; 12(1): 5206. <http://doi.org/10.1038/s41467-021-25541-3> PMID: 34471126.
11. Patinios C, Creutzburg SCA, Arifah AQ, Adiego-Perez B, Gyimah EA, Ingham CJ, et al. Streamlined CRISPR genome engineering in wild-type bacteria using SIBR-Cas. *Nucleic Acids Res*. 2021; 49(19): 11392–11404. <http://doi.org/10.1093/nar/gkab893> PMID: 34614191.
12. Chen W, Ren ZH, Tang N, Chai G, Zhang H, Zhang Y, et al. Targeted genetic screening in bacteria with a Cas12k-guided transposase. *Cell Rep*. 2021; 36(9): 109635. <http://doi.org/10.1016/j.celrep.2021.109635> PMID: 34469724.
13. Xu Z, Li Y, Cao H, Si M, Zhang G, Woo PCY, et al. A transferrable and integrative type I-F Cascade for heterologous genome editing and transcription modulation. *Nucleic Acids Res*. 2021; 49(16): e94. <http://doi.org/10.1093/nar/gkab521> PMID: 34157103.
14. Yan MY, Li SS, Ding XY, Guo XP, Jin Q, Sun YC. A CRISPR-assisted nonhomologous end-joining strategy for efficient genome editing in *Mycobacterium tuberculosis*. *mBio*. 2020; 11(1): e02364–19. <http://doi.org/10.1128/mBio.02364-19> PMID: 31992616.
15. Zocca VFB, Correa GG, Lins M, de Jesus VN, Tavares LF, Amorim L, et al. The CRISPR toolbox for the gram-positive model bacterium *Bacillus subtilis*. *Crit Rev Biotechnol*. 2022; 42(6): 813–826. <http://doi.org/10.1080/07388551.2021.1983516> PMID: 34719304.
16. Zhao XC, Chen X, Xue YB, Wang XD. Development of an efficient iterative genome editing method in *Bacillus subtilis* using the CRISPR-AsCpf1 system. *J Basic Microb*. 2022; 62(7): 824–832. <http://doi.org/10.1002/jobm.202200134> PMID: 35655368.
17. Jiang Y, Qian F, Yang J, Liu Y, Dong F, Xu C, et al. CRISPR-Cpf1 assisted genome editing of *Corynebacterium glutamicum*. *Nat Commun*. 2017; 8: 15179. <http://doi.org/10.1038/ncomms15179> PMID: 28469274.



18. Fedorova I, Arseniev A, Selkova P, Pobegalov G, Goryanin I, Vasileva A, et al. DNA targeting by *Clostridium cellulolyticum* CRISPR-Cas9 Type II-C system. *Nucleic Acids Res.* 2020; 48(4): 2026–2034. <http://doi.org/10.1093/nar/gkz1225> PMID: 31943070.
19. Tong Y, Whitford CM, Blin K, Jorgensen TS, Weber T, Lee SY. CRISPR-Cas9, CRISPRi and CRISPR-BEST-mediated genetic manipulation in streptomycetes. *Nat Protoc.* 2020; 15(8): 2470–2502. <http://doi.org/10.1038/s41596-020-0339-z> PMID: 32651565.
20. Chen Y, Cheng M, Feng X, Niu X, Song H, Cao Y. Genome editing by CRISPR/Cas12 recognizing AT-rich PAMs in *Shewanella oneidensis* MR-1. *ACS Synth Biol.* 2022; 11(9): 2947–2955. <http://doi.org/10.1021/acssynbio.2c00208> PMID: 36048424.
21. Halperin SO, Tou CJ, Wong EB, Modavi C, Schaffer DV, Dueber JE. CRISPR-guided DNA polymerases enable diversification of all nucleotides in a tunable window. *Nature.* 2018; 560(7717): 248–252. <http://doi.org/10.1038/s41586-018-0384-8> PMID: 30069054.
22. Liu ZQ, Dong HN, Cui YL, Cong LN, Zhang DW. Application of different types of CRISPR/Cas-based systems in bacteria. *Microb Cell Fact.* 2020; 19(1): 172. <http://doi.org/10.1186/s12934-020-01431-z> PMID: 32883277.
23. Teufel M, Klein CA, Mager M, Sobetzko P. A multifunctional system for genome editing and large-scale interspecies gene transfer. *Nat Commun.* 2022; 13(1): 3430. <http://doi.org/10.1038/s41467-022-30843-1> PMID: 35701417.
24. Zetsche B, Gootenberg JS, Abudayyeh OO, Slaymaker IM, Makarova KS, Essletzbichler P, et al. Cpf1 is a single RNA-guided endonuclease of a class 2 CRISPR-Cas system. *Cell.* 2015; 163(3): 759–771. <http://doi.org/10.1016/j.cell.2015.09.038> PMID: 26422227.
25. Csorgo B, Leon LM, Chau-Ly IJ, Vasquez-Rifo A, Berry JD, Mahendra C, et al. A compact Cascade-Cas3 system for targeted genome engineering. *Nat Methods.* 2020; 17(12): 1183–1190. <http://doi.org/10.1038/s41592-020-00980-w> PMID: 33077967.
26. Hidalgo-Cantabrana C, Goh YJ, Pan MC, Sanozky-Dawes R, Barrangou R. Genome editing using the endogenous type I CRISPR-Cas system in *Lactobacillus crispatus*. *Proc Natl Acad Sci U S A.* 2019; 116(32): 15774–15783. <http://doi.org/10.1073/pnas.1905421116> PMID: 31341082.
27. Pan M, Morovic W, Hidalgo-Cantabrana C, Roberts A, Walden KKO, Goh YJ, et al. Genomic and epigenetic landscapes drive CRISPR-based genome editing in *Bifidobacterium*. *Proc Natl Acad Sci U S A.* 2022; 119(30): e2205068119. <http://doi.org/10.1073/pnas.2205068119> PMID: 35857876.
28. Ayora S, Carrasco B, Cardenas PP, Cesar CE, Canas C, Yadav T, et al. Double-strand break repair in bacteria: a view from *Bacillus subtilis*. *FEMS Microbiol Rev.* 2011; 35(6): 1055–1081. <http://doi.org/10.1111/j.1574-6976.2011.00272.x> PMID: 21517913.
29. Vercoe RB, Chang JT, Dy RL, Taylor C, Gristwood T, Clulow JS, et al. Cytotoxic chromosomal targeting by CRISPR/Cas systems can reshape bacterial genomes and expel or remodel pathogenicity islands. *PLoS Genet.* 2013; 9(4): e1003454. <http://doi.org/10.1371/journal.pgen.1003454> PMID: 23637624.
30. Zhou Y, Liu X, Wu J, Zhao G, Wang J. CRISPR-Cas12a-assisted genome editing in *Amycolatopsis mediterranei*. *Front Bioeng Biotechnol.* 2020; 8:698. <http://doi.org/10.3389/fbioe.2020.00698> PMID: 32671053.
31. Amare B, Mo A, Khan N, Sowa DJ, Warner MM, Tetenyh A, et al. LigD: a structural guide to the multi-tool of bacterial non-homologous end joining. *Front Mol Biosci.* 2021; 8: 787709. <http://doi.org/10.3389/fmolb.2021.787709> PMID: 34901162.
32. Malyarchuk S, Wright D, Castore R, Klepper E, Weiss B, Doherty AJ, et al. Expression of *Mycobacterium tuberculosis* ku and ligase D in *Escherichia coli* results in RecA and RecB-independent DNA end-joining at regions of microhomology. *DNA Repair.* 2007; 6(10): 1413–1424. <http://doi.org/10.1016/j.dnarep.2007.04.004> PMID: 17560174.
33. Chayot R, Montagne B, Mazel D, Ricchetti M. An end-joining repair mechanism in *Escherichia coli*. *Proc Natl Acad Sci U S A.* 2010; 107(5): 2141–2146. <http://doi.org/10.1073/pnas.0906355107> PMID: 20133858.
34. Midha S, Bansal K, Kumar S, Giriya AM, Mishra D, Brahma K, et al. Population genomic insights into variation and evolution of *Xanthomonas oryzae* pv. *oryzae*. *Sci Rep.* 2017; 7: 40694. <http://doi.org/10.1038/srep40694> PMID: 28084432.
35. Salzberg SL, Sommer DD, Schatz MC, Phillippy AM, Rabinowicz PD, Tsuge S, et al. Genome sequence and rapid evolution of the rice pathogen *Xanthomonas oryzae* pv. *oryzae* PXO99<sup>A</sup>. *BMC Genomics.* 2008; 9: 204. <http://doi.org/10.1186/1471-2164-9-204> PMID: 18452608.
36. Liu QB, Wang SW, Long JY, Chen ZY, Yang B, Lin F. Functional identification of the *Xanthomonas oryzae* pv. *oryzae* Type I-C CRISPR-Cas system and its potential in gene editing application. *Front Microbiol.* 2021; 12: 686715. <http://doi.org/10.3389/Fmicb.2021.686715> PMID: 34475857.

37. Jiang DD, Zhang DD, Li SN, Liang YT, Zhang QW, Qin X, et al. Highly efficient genome editing in *Xanthomonas oryzae* pv. *oryzae* through repurposing the endogenous type I-C CRISPR-Cas system. *Mol Plant Pathol*. 2022; 23(4): 583–594. <http://doi.org/10.1111/mpp.13178> PMID: 34954876.
38. Yang FY, Wei N, Zhang ZH, Wang M, Liu YC, Zhang LF, et al. Genome editing of *Corynebacterium glutamicum* mediated with Cpf1 plus Ku/LigD. *Biotechnol Lett*. 2021; 43(12): 2273–2281. <http://doi.org/10.1007/s10529-021-03195-x> PMID: 34669078.
39. Fu YF, Sander JD, Reyon D, Cascio VM, Joung JK. Improving CRISPR-Cas nuclease specificity using truncated guide RNAs. *Nat Biotechnol*. 2014; 32(3): 279–284. <http://doi.org/10.1038/nbt.2808> PMID: 24463574.
40. Ming ML, Ren QR, Pan CT, He Y, Zhang YX, Liu SS, et al. CRISPR-Cas12b enables efficient plant genome engineering. *Nat Plants*. 2020; 6(3): 202–208. <http://doi.org/10.1038/s41477-020-0614-6> PMID: 32170285.
41. Wang SF, Sun JH, Fan FG, Tan ZY, Zou YM, Lu DP. A *Xanthomonas oryzae* pv. *oryzae* effector, XopR, associates with receptor-like cytoplasmic kinases and suppresses PAMP-triggered stomatal closure. *Sci China Life Sci*. 2016; 59(9): 897–905. <http://doi.org/10.1007/s11427-016-5106-6> PMID: 27520828.
42. Yamaguchi K, Yamada K, Ishikawa K, Yoshimura S, Hayashi N, Uchihashi K, et al. A receptor-like cytoplasmic kinase targeted by a plant pathogen effector is directly phosphorylated by the chitin receptor and mediates rice immunity. *Cell Host Microbe*. 2013; 13(3): 347–57. <http://doi.org/10.1016/j.chom.2013.02.007> PMID: 23498959.
43. Ishikawa K, Yamaguchi K, Sakamoto K, Yoshimura S, Inoue K, Tsuge S, et al. Bacterial effector modulation of host E3 ligase activity suppresses PAMP-triggered immunity in rice. *Nat Commun*. 2014; 5: 5430. <http://doi.org/10.1038/ncomms6430> PMID: 25388636.
44. Booher NJ, Carpenter SCD, Sebra RP, Wang L, Salzberg SL, Leach JE, et al. Single molecule real-time sequencing of *Xanthomonas oryzae* genomes reveals a dynamic structure and complex TAL (transcription activator-like) effector gene relationships. *Microb Genom*. 2015; 1(4): e000032. <http://doi.org/10.1099/Mgen.0.000032> PMID: 27148456.
45. Zou L, Li Y, Chen G. A non-marker mutagenesis strategy to generate poly-hrp gene mutants in the rice pathogen *Xanthomonas oryzae* pv. *oryzicola*. *Agri Sci China*. 2011; 10(8): 1139–1150. [http://doi.org/10.1016/S1671-2927\(11\)60104-1](http://doi.org/10.1016/S1671-2927(11)60104-1).
46. Song C, Yang B. Mutagenesis of 18 type III effectors reveals virulence function of XopZ(PXO99) in *Xanthomonas oryzae* pv. *oryzae*. *Mol Plant Microbe Interact*. 2010; 23(7): 893–902. <http://doi.org/10.1094/MPMI-23-7-0893> PMID: 20521952.
47. Ren B, Yan F, Kuang YJ, Li N, Zhang DW, Zhou XP, et al. Improved base editor for efficiently inducing genetic variations in rice with CRISPR/Cas9-guided hyperactive hAID mutant. *Mol Plant*. 2018; 11(4): 623–626. <http://doi.org/10.1016/j.molp.2018.01.005> PMID: 29382569.
48. Komor AC, Kim YB, Packer MS, Zuris JA, Liu DR. Programmable editing of a target base in genomic DNA without double-stranded DNA cleavage. *Nature*. 2016; 533(7603): 420–424. <http://doi.org/10.1038/nature17946> PMID: 27096365.
49. Chen WZ, Zhang Y, Zhang YF, Pi YS, Gu TN, Song LQ, et al. CRISPR/Cas9-based genome editing in *Pseudomonas aeruginosa* and cytidine deaminase-mediated base editing in *Pseudomonas* species. *iScience*. 2018; 6: 222–231. <http://doi.org/10.1016/j.isci.2018.07.024> PMID: 30240613.
50. Ho J, Zhao M, Wojcik S, Taiaroa G, Butler M, Poulter R. The application of the CRISPR-Cas9 system in *Pseudomonas syringae* pv. *actinidiae*. *J Med Microbiol*. 2020; 69(3): 478–486. <http://doi.org/10.1099/jmm.0.001124> PMID: 31935181.
51. Yue SJ, Huang P, Li S, Cai YY, Wang W, Zhang XH, et al. Developing a CRISPR-assisted base-editing system for genome engineering of *Pseudomonas chlororaphis*. *Microb Biotechnol*. 2022; 15(9): 2324–2336. <http://doi.org/10.1111/1751-7915.14075> PMID: 35575623.
52. Rodrigues SD, Karimi M, Impens L, Van Lerberge E, Coussens G, Aesaert S, et al. Efficient CRISPR-mediated base editing in *Agrobacterium* spp. *Proc Natl Acad Sci U S A*. 2021; 118(2): e2013338118. <http://doi.org/10.1073/pnas.2013338118> PMID: 33443212.
53. Parcey M, Gayder S, Castle AJ, Svircev AM. Function and application of the CRISPR-Cas system in the plant pathogen *Erwinia amylovora*. *Appl Environ Microbiol*. 2022; 88(7): e0251321. <http://doi.org/10.1128/aem.02513-21> PMID: 35285707.
54. Cain AK, Barquist L, Goodman AL, Paulsen IT, Parkhill J, van Opijnen T. A decade of advances in transposon-insertion sequencing. *Nat Rev Genet*. 2020; 21(9): 526–540. <http://doi.org/10.1038/s41576-020-0244-x> PMID: 32533119.
55. Green B, Bouchier C, Fairhead C, Craig NL, Cormack BP. Insertion site preference of Mu, Tn5, and Tn7 transposons. *Mob DNA*. 2012; 3(1): 3. <http://doi.org/10.1186/1759-8753-3-3> PMID: 22313799.

56. Sun Q, Wu W, Qian W, Hu J, Fang R, He C. High-quality mutant libraries of *Xanthomonas oryzae* pv. *oryzae* and *X. campestris* pv. *campestris* generated by an efficient transposon mutagenesis system. *FEMS Microbiol Lett.* 2003; 226(1): 145–150. [http://doi.org/10.1016/S0378-1097\(03\)00583-4](http://doi.org/10.1016/S0378-1097(03)00583-4) PMID: 13129620.
57. Callando BJ, Voigt CA. Targeted DNA degradation using a CRISPR device stably carried in the host genome. *Nat Commun.* 2015; 6: 6989. <http://doi.org/10.1038/Ncomms7989> PMID: 25988366.
58. Hamilton TA, Pellegrino GM, Therrien JA, Ham DT, Bartlett PC, Karas BJ, et al. Efficient inter-species conjugative transfer of a CRISPR nuclease for targeted bacterial killing. *Nat Commun.* 2019; 10(1): 4544. <http://doi.org/10.1038/S41467-019-12448-3> PMID: 31586051.
59. Li H, Durbin R. Fast and accurate long-read alignment with Burrows-Wheeler transform. *Bioinformatics.* 2010; 26(5): 589–595. <http://doi.org/10.1093/bioinformatics/btp698> PMID: 20080505.
60. Danecek P, Bonfield JK, Liddle J, Marshall J, Ohan V, Pollard MO, et al. Twelve years of SAMtools and BCFtools. *GigaScience.* 2021; 10(2): giab008. <http://doi.org/10.1093/gigascience/giab008> PMID: 33590861.
61. DePristo MA, Banks E, Poplin R, Garimella KV, Maguire JR, Hartl C, et al. A framework for variation discovery and genotyping using next-generation DNA sequencing data. *Nat Genet.* 2011; 43(5): 491–498. <http://doi.org/10.1038/ng.806> PMID: 21478889.
62. Wilm A, Aw PPK, Bertrand D, Yeo GHT, Ong SH, Wong CH, et al. LoFreq: a sequence-quality aware, ultra-sensitive variant caller for uncovering cell-population heterogeneity from high-throughput sequencing datasets. *Nucleic Acids Res.* 2012; 40(22): 11189–11201. <http://doi.org/10.1093/nar/gks918> PMID: 23066108.
63. Kim S, Scheffler K, Halpern AL, Bekritsky MA, Noh E, Kallberg M, et al. Strelka2: fast and accurate calling of germline and somatic variants. *Nat Methods.* 2018; 15(8): 591–594. <http://doi.org/10.1038/s41592-018-0051-x> PMID: 30013048.
64. Robinson JT, Thorvaldsdottir H, Winckler W, Guttman M, Lander ES, Getz G, et al. Integrative genomics viewer. *Nat Biotechnol.* 2011; 29(1): 24–26. <http://doi.org/10.1038/nbt.1754> PMID: 21221095.